DETECTION OF NH_3 MOLECULES IN THE INTERSTELLAR MEDIUM BY THEIR MICROWAVE EMISSION*

A. C. Cheung, D. M. Rank, and C. H. Townes
Department of Physics, University of California, Berkeley, California

and

D. D. Thornton and W. J. Welch
Radio Astronomy Laboratory, Space Sciences Laboratory, and Department of Electrical Engineering, University of California, Berkeley, California

(Received 15 November 1968)

Ammonia has been found in the direction of the galactic center by detection of its $J=1$, $K=1$ inversion transition. The region of emission closely corresponds to the position, velocity, and size of strong OH absorption. Collisional and radiative excitation mechanisms are discussed. The column density of NH_3 and the kinetic temperature of the interstellar gas cloud are estimated to be $2\times10^{16}/cm^2$ and 23°K, respectively.

Ammonia molecules have been detected in the interstellar medium with a new 20-ft radio telescope operating at a wavelength of 1.25 cm. Line emission was observed at a frequency corresponding to the inversion transitions of the $J=1$, $K=1$ rotational level in the vibrational ground state of the NH_3 molecule. Figure 1 shows the pertinent energy levels of the NH_3 molecule, including hyperfine structure.

The emission region is of small angular extent and is displaced to the south from the direction of the galactic center by 3 ± 2 min arc. The radiation most probably originates in a dense cloud of 3′ angular diameter in which strong OH absorption has been observed.[1] Weaker emission from the inversion transition of the $J=2, K=2$ state from this same region seems also to be present, although in this case the signal-to-noise ratio is not large. The (1,1) inversion radiation has an antenna temperature of $T_A(1,1)=0.46\pm0.05$°K, a linewidth of about 2 MHz, and a Doppler frequency shift corresponding to an average velocity of +23 km/sec with respect to the local standard of rest. The error given is the standard deviation calculated from fluctuations in the observations. Emission from the (2,2) inversion transition yields an antenna temperature $T_A(2,2)=0.16\pm0.05$°K with a similar width and Doppler shift.

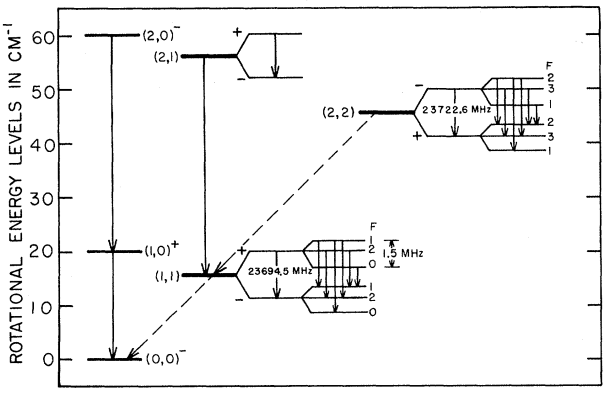

FIG. 1. Energy level diagram of the NH_3 molecule in its ground vibrational state. The scale for the inversion levels is 10 times the scale for rotational energy, and hyperfine splittings are magnified by 10^4. Electric dipole transitions are indicated by the solid arrows.

The main component of the apparatus is the 20-ft diam millimeter-wavelength antenna which was recently put into operation at the Hat Creek Station of the University of California's Radio Astronomy Laboratory. The properties of this antenna and its associated receiving equipment will be described in detail elsewhere[2] and only summarized here. The aperture efficiency is 60% at 23.6 GHz, corresponding to a gain of $1.3\times10^{+6}$, and the pattern is symmetric with half-power width 8.5′. The antenna can be repositioned with an angular accuracy of 0.25′. For the measurements reported in the Letter, we believe that the absolute inaccuracy of the antenna pointing does not exceed 1.0′. In addition to the main feed horn at the Cassegrain focus, there is an off-axis reference horn providing a reference beam displaced by 19.8′ from the main beam. The gain in the reference beam is about 15% less than than of the main beam.

A Dicke radiometer, using the reference beam for comparison, is coupled to the antenna. The basic receiver in the radiometer has a balanced mixer with a double-channel noise temperature of about 2000°K. The output of the main i.f. am-

plifier goes into the eight filter-detector elements of the multichannel receiver. Any one of four sets of filters with widths ranging from 0.35 to 50 MHz may be used. 1.25-MHz filters were used for the results reported here. The filter outputs are recorded continuously. Calibration of the radiometer is effected by turning on a plasma discharge tube which is weakly coupled to the radiometer input, the intensity of this input signal having been previously calibrated against blackbody sources in the laboratory. The local oscillator is a backward-wave tube which is stabilized to about one part in 10^6 on a frequency synthesizer.

The basic observation routine consists of tracking the radio source first in the main beam and then in the reference beam, recording the radiometer outputs during both intervals, and taking the difference between the two sets of outputs. The observations are sequenced so that the antenna tracks through the same hour angles for both intervals. This assures that the effects of systematic pickup from the ground and atmosphere are canceled. The movement of the antenna, introduction of the "calibrate" signal, and recording of data in sequence are all controlled by a PDP-8/S computer. A complete observation run consists of one recording of the "calibrate" signal followed by eight alternate observations in the main and reference beams. At the end of such a run, the computer calculates the average antenna temperature of the radio source normalized to the known "calibrate" signal and the standard deviation among the 16 recording intervals for each channel and then types out these eight averages and eight standard deviations. Spectra such as those shown in Fig. 2 were obtained by taking the weighted average of a number of these runs.

Figure 2(a) shows the observed spectrum, at the (1, 1) inversion frequency, of a region approximately 8.5′ in diameter centered on the position marked by a triangle in Fig. 3(c). The ordinate of Fig. 2 corresponds to the temperature of only one of the two sidebands of the receiver. The continuum temperature should be scaled down by a factor of 2 since it is also received in the image sideband. The spectral range of Fig. 2(a) extends from −82 to +150 km/sec with a resolution of about 15 km/sec. For comparison, the vertical lines underneath the emission feature in Fig. 2(a) represent the relative positions and intensities of the hyperfine components of the (1, 1) line. The numbers across the top of the

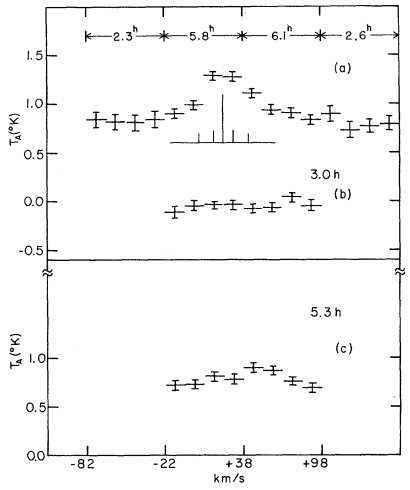

FIG. 2. Observed NH_3 spectra and continuum from the galactic center. (a) $J=1, K=1$ inversion of NH_3 with the expected hyperfine splitting superimposed, (b) baseline from empty sky, and (c) $J=2, K=2$ inversion line of NH_3. The continuum temperature should be scaled down by a factor of 2 because superheterodyne detection accepts both sidebands of continuum radiation.

figure are the total integration times in hours for the corresponding filter positions. The variation of integration time for filter positions in groups of four instead of groups of eight resulted from tests performed to verify the actual frequency and reproducibility of the line by means of overlapping measurements with different local oscillator frequencies.

Figure 2(b) shows a baseline taken on blank sky at the same declination as the galactic center. Figure 2(c) is the spectrum obtained by pointing toward the position marked by the triangle on the map in Fig. 3(c) at the (2, 2) inversion frequency of NH_3. The detection of the (2, 2) line is clearly not as certain as that of the (1, 1) line. The peak emission in Fig. 2(c), corresponding to a Doppler velocity of about 50 km/sec, has a signal-to-noise ratio of about 3:1. Nonetheless, this represents a level of confidence over 95%. The apparent difference in velocity between the two features in 2(a) and 2(c) could be due to the low signal-to-noise ratio for the (2, 2) line or to differences in temperature within the emission region. The linewidth of the (1, 1) transition is consistent with about 25 km/sec of turbulent broadening after hyperfine structure and instrumental resolution are considered.

Additional observations of the intensity of the (1, 1) inversion line were made at the positions marked by crosses on the map in Fig. 3(c). Re-

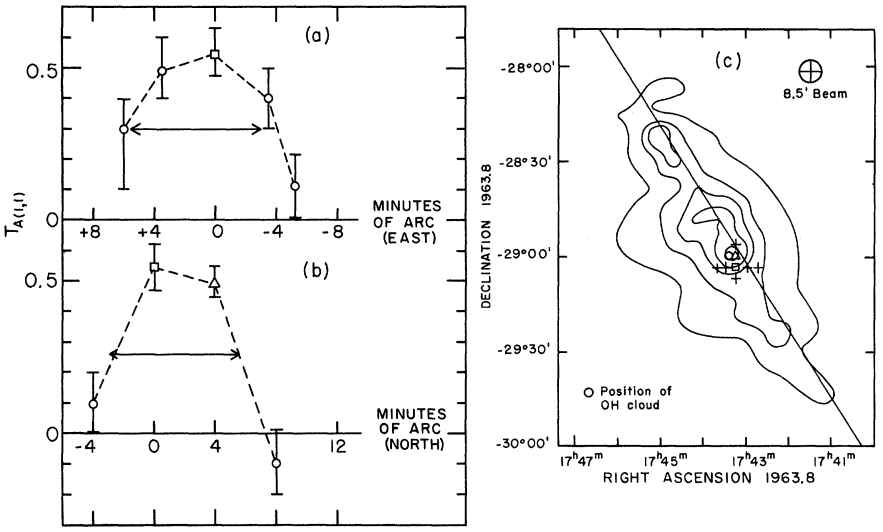

FIG. 3. Distribution of NH_3 in the direction of the galactic center. The NH_3 cloud is displaced $-3' \pm 2'$ in declination and $0'' \pm 9''$ in right ascension from the bright radio center. (a) Profile of (1, 1) NH_3 emission in right ascension, (b) profile of NH_3 emission in declination, and (c) 5-GHz map [see N. W. Broten et al., Australian J. Phys. 18, 85 (1965)] of Sagittarius A showing the region scanned in (a) and (b).

sults of these measurements showing the angular extent of NH_3 emission are summarized in Figs. 3(a) and 3(b). An arrow on each of these two figures indicates the half-power beamwidth of our antenna. These measurements limit the source size for the (1, 1) line emission to <5'.

Our identification of these emission lines with NH_3 molecules in the interstellar medium rests on the close coincidence of the emission feature in Fig. 2(a) with the (1, 1) inversion transition of NH_3. It is further supported by (a) the probable detection of the (2, 2) transition as shown in Fig. 2(c) and (b) the close correspondence in both Doppler shift and turbulent width of the (1, 1) emission with the OH absorption feature in roughly the same direction.[3] Production of this line emission by some constituent of the galaxy other than NH_3 gas is very improbable because we find no other reasonable line from molecules[4] or recombination spectra which could explain the observations.

The possibility that this emission comes from the earth's atmosphere can be ruled out for a number of reasons: (a) Any emission from the atmosphere is cancelled by the technique of switching between two feed horns, (b) atmospheric NH_3 emission would have a velocity of −17 km/sec in Fig. 2(a), and (c) pressure broadening of NH_3 lines in the atmosphere makes them undetectable in the present experiment.

The observed line intensities may be used to estimate both the column density of NH_3 and the kinetic temperature of the interstellar gas cloud. Since $\Delta K \neq 0$ transitions are forbidden in electric dipole or quadrupole radiation, the principal source of radiation of both the (1, 1) and (2, 2) levels to lower rotational states appears to be the nuclear magnetic dipoles of hydrogen; the spontaneous emission lifetime due to these is at least as long as 10^{13} sec. The ground rotational state (0, 0) shows no inversion, and this long radiative lifetime for the $K = J$ excited states explains why the inversion spectrum might be expected from interstellar space.[5] The decay time for $\Delta K \neq 0$ by radiative processes is very slow compared with collisions between NH_3 molecules and neutral hydrogen, which have mean times between collisions of about $10^{10}/n_H$ sec, where n_H is the number of H atoms or molecules. n_H is probable as large as unity, so that transitions between the rotational states (0, 0), (1, 1), and (2, 2) are primarily due to collisions, and their relative populations should be determined by the kinetic temperature of the gas T_{kin}.

Since the observed radiation at the inversion frequencies is more intense than the Sagittarius A microwave continuum, the inversion-level population must not be in equilibrium with this microwave field but rather is affected by other processes which produce a higher effective temperature. Radiative transitions induced by the isotropic microwave continuum at 2.7°K would make

the (1, 1) and (2, 2) inversion levels approach equilibrium with a time constant of about 6×10^6 sec. Hence excitation, presumably due to collision with H atoms or molecules, must occur at a comparable rate or faster. From this, one obtains $n_H \gtrsim 10^3$, most of which is probably in the molecular state. Electrons, if they are present, have both a higher cross section for excitation of inversion and a higher velocity than does neutral hydrogen, so that the time between excitation by electrons is about $10^6/n_e$, where n_e is the electron density. Thus an electron density as large as 10^{-1} rather than $n_H \gtrsim 10^3$ could produce the needed excitation, but it seems unlikely that the NH_3 exists in the presence of such ionization.

The ratio of (1, 1) and (2, 2) intensities depends only on the matrix elements and the relative population of the two rotational states, if the optical depth for the NH_3 emission is not too large. The observed ratio of antenna temperatures, $\int T_B(2, 2)d\nu / \int T_B(1,1)d\nu = 0.34 \pm 0.10$, thus determines the gas kinetic temperature to be $T_{kin} = 23 \pm 5°K$.

The integrated intensity of the emission line gives a lower limit for the number of molecules per unit area seen by the telescope and, if the cloud of NH_3 is not optically thick, this number can be evaluated. For an optically thin cloud, the integrated intensity $\int T_B d\nu = (8\pi^3 Nf/3ck)(\mu_{JK})^2 \nu_{JK}{}^2 L$ where N = total density of NH_3 molecules in all states, f = fraction of total molecules in a single inversion level of a particular rotational state (J, K), and $(\mu_{JK})^2$ = matrix element for the transition $= [K^2/J(J+1)]\mu^2$, with μ the molecular dipole moment. c and k are the velocity of light and Boltzmann's constant, and L = distance through the cloud along the line of sight.

If the cloud's angular size is assumed to be 3′, about the same size as the region of strong OH absorption, the filling factor of the antenna is 18. Since the mean atmospheric absorption was measured to be 30% at the declination angle of −29°, the disk brightness temperature of the cloud is 11°K above the continuum background. If one takes $T_{kin} = 23°K$ as determined above, then the optical depth is about 0.7. The optical depth cannot be great because the (2, 2) emission temperature is appreciably less than that of the (1, 1) transition. From the above expression for integrated intensity, one obtains for the column density of NH_3 molecules in all states $NL = 2\times10^{16}/cm^2$ in the line of sight. Both the column density and optical depth are estimates only, the uncertainty arising mainly from the cloud size. In any case, the cloud should not be smaller than about 2′ because this would raise the brightness temperature T_B to 23°K, the maximum temperature which can be produced by collisions. For a uniform cloud of length 10 lt yr, the density of NH_3 molecules would be 10^{-3} cm^{-3}. With a hydrogen density of 10^3 cm^{-3} and the cosmic ratio of nitrogen to hydrogen (10^{-4}), one concludes that a substantial fraction, perhaps 1%, of the total nitrogen is in the form of NH_3.

Detailed calculations, including a significant optical depth of the NH_3 cloud and transmission through it of the microwave background from Sagittarius A, are consistent with the data for a temperature range $17° < T_{kin} < 30°K$ and an optical depth for the (1, 1) transition between 0.5 and 3. This assumes that distributions in the $J=K$ rotational and inversion states are all determined by the same temperature. Until additional information is available on the cloud size, position, and line intensities, more precise calculations than those obtained from the simple model above do not seem justified.

Since NH_3 is a fairly complex molecule, it is most likely formed by adsorbed N and H atoms on interstellar grain surfaces rather than by successive binary collisions. If NH_3 molecules are formed in this manner, the large quantities of NH_3 which we have observed must be driven off the grain surfaces by sublimation, photodetachment, or possibly particle bombardment. Once formed, NH_3 molecules will be subject to destruction by ultraviolet photons. The photodissociation cross section for NH_3 is 3.7×10^{-18} cm^2/uv photon.[6] Assuming the average flux of uv photons with $\lambda < 2000$ Å to be 10^8/cm^2 sec in interstellar starlight, the lifetime of NH_3 is about 10^2 yr. The lifetime of NH_3 inside a dust cloud will be many orders of magnitude larger than this since uv absorption by the dust grains and molecules at the edges of the cloud will protect the interior.

We have also searched for NH_3 emission or absorption in a number of other sources, including Cassiopeia A, W51, NML Cygnus, and a few other dense dust clouds with as yet no further success. NH_3 can be expected in other areas of the galaxy in which OH and large amounts of dust are seen. The study of NH_3 transitions should be a sensitive means of determining kinetic temperatures and yield a variety of other information about these relatively cool regions of interstellar gas and dust grains.

We would like to thank H. Weaver, C. Heiles, N. Dieter, and P. Swings for many instructive

discussions during the course of this work, and P. Rhodes for helping with the observations.

*Work supported in part by the National Aeronautics and Space Administration, Office of Naval Research, and the National Science Foundation.

[1]H. F. Weaver, P. Baker, and R. E. Hills, to be published.

[2]D. D. Thornton and W. J. Welch, to be published.

[3]D. R. W. Williams, presented at URSI-IEEE Spring Meeting, Washington, D. C. 20-23 April, 1965 (unpublished).

[4]Microwave Spectral Tables (National Bureau of Standards, Washington, D.C., 1968), Vol. V.

[5]C. H. Townes, in the Fourth International Astronomical Union Symposium, Manchester, England, 1955, edited by H. C. Van de Hulst (Cambridge University Press, Cambridge, 1957), Paper 16.

[6]A. E. Potter and B. Del Duca, Icarus 3, 103 (1964).

EVIDENCE FOR THE $K_1^0K_1^0$ ENHANCEMENT NEAR THRESHOLD PRODUCED BY K^-N INTERACTIONS*

Jean Alitti,† Virgil E. Barnes, David J. Crennell, Enzo Flaminio, Marvin Goldberg,‡ Uri Karshon,§ Kwan Wu Lai, Wesley J. Metzger,‖ John S. O'Neall, Nicholas P. Samios, J. Michael Scarr, and Thomas G. Schumann**

Physics Department, Brookhaven National Laboratory, Upton, New York 11973

A $J^{PC}=0^{++}$ $K_1^0K_1^0$ enhancement at a mass of 1030 ± 10 MeV with a width of 45^{+35}_{-15} MeV is observed in $\bar{K}N$ interactions. An s-wave resonance interpretation of this enhancement is favored over an s-wave scattering length effect. Within experimental uncertainties, we associate this enhancement with the S^* observed in π^-p interactions.

The experimental evidence for an isosinglet, scalar $K_1^0K_1^0$ enhancement ($I^G=0^+$, $J^P=0^+$) comes mainly from a study of the reaction $\pi^-p\rightarrow K_1^0K_1^0n$ at pion momenta from 2 to 12 GeV/c.[1] Because the enhancement is near the $K\bar{K}$ threshold the available data can be interpreted either in terms of an s-wave resonance or a simple s-wave complex scattering length.[2] The resonance interpretation, namely the S^* with mass $M=1069\pm10$ MeV and width $\Gamma=72\pm14$ MeV, is favored by the experiments with incident pions of 5, 6, 7, and 12 GeV/c,[3] whereas the scattering-length fit is favored by the experiment at 2.0 GeV/c.[4] In some cases, such as the experiments at 4 and 5 GeV/c, either interpretation can be used to describe the data.[5] In addition, an $I=1K\bar{K}$ enhancement near threshold, π_N(1016 MeV), has been observed in the reaction $\bar{p}p\rightarrow K^\pm K_1^0\pi^\mp$ at rest.[6] This effect has been related to the $\delta^\pm$(975) boson resonance[7] below the $K\bar{K}$ threshold.[8]

Data for this study come from a number of exposures of the Brookhaven National Laboratory (BNL) 80-in. bubble chamber filled separately with liquid hydrogen and deuterium to separated beams of K^- mesons at 3.6, 3.9, 4.65, and 5.0 GeV/c. A further breakdown concerning the exposures is shown in Table I.

The reaction of interest in this study was $K^-N\rightarrow K_1^0K_1^0$(MM), where N was either a proton or neutron and the missing mass (MM) was equal to or greater than that of the Λ^0 hyperon.[9] The main requirement was that both K_1^0's decay in the chamber via their visible decay modes $K_1^0\rightarrow\pi^+\pi^-$. The criteria for the identification of the K_1^0 were that: (1) the K_1^0 decay make a satisfactory three-constraint fit to the production vertex, this being defined by a $\chi^2\leq12$; (2) the ionization of the π^+ and π^- from the decaying K_1^0 be consistent with that expected from the kinematic fit; and (3) in the case of a Λ^0,K^0 ambiguity, the K^0 interpretation be omitted from the sample[10] because Λ^0's can often be fitted as K_1^0's but the opposite is not often the case.

In Fig. 1(a) is plotted the $K_1^0K_1^0$ mass distribution for this sample of 568 events. Marked enhancements are evident near the $K\bar{K}$ threshold (1030 MeV) and at the well-known f^* resonance (1515 MeV). These regions are indicated in the figure. The cross-hatched events in Fig. 1(a)

Table I. A detailed breakdown of the exposures of the BNL 80-in. liquid-filled bubble chamber to separated beams of K^- mesons.

Beam momentum	Liquid	Events/μb nucleon
3.6	Deuterium	10
3.9	Deuterium	40
3.9	Hydrogen	10
4.65	Hydrogen	15
5.0	Hydrogen	5
Total		80